NON-EQUILIBRIUM ESCAPE PROBLEMS UNDER BIVARIATE α-STABLE NOISES

Bartłomiej Dybiec, Krzysztof Szczepaniec

The Marian Smoluchowski Institute of Physics
and
Mark Kac Center for Complex Systems Research, Institute of Physics
Jagiellonian University, Łojasiewicza 11, 30-348 Kraków, Poland

Igor M. Sokolov

Institut für Physik, Humboldt Universität zu Berlin
Newtonstr. 15, 12489 Berlin, Germany

(Received February 11, 2016; revised version received March 17, 2016)

Stochastic resonance is a prominent effect consisting in enhancement of a response of a physical system to deterministic driving in the presence of noise. It demonstrates a constructive role the noise may play in increasing the sensitivity of the system to weak signals, and emerges in different theoretical models and experimental situations. We consider this effect in a periodically modulated two-dimensional double-well potential under the influence of an isotropic α-stable noise, and discuss the performance of various measures used to describe the stochastic resonance in other setups.

DOI:10.5506/APhysPolB.47.1327

1. Introduction

Stochastic resonance [1–4], next to resonant activation [5], noise enhanced stability [6] and stochastic synchronization [7] is the most prominent noise induced effect. Theory of the stochastic resonance intuitively explains how noise can be used to enhance weak signals. In particular, it has been suggested that occurrence of ice ages can be justified by this celebrated phenomenon [8, 9]. Stochastic resonance has far-reaching biological implications [10–12] and medical applications [13–16].

Stochastic resonance (SR) is an effect in which an optimal amount of noise synchronizes and amplifies system's response. Minimal SR setup consists of a Brownian particle moving in a periodically modulated double-well

potential. Noise present in the system, originating due to large number of collisions of a test particle with its thermal bath, is an important model component. Noise-induced barrier crossing events are crucial for occurrence of SR. Typically, it is assumed that noise is white and Gaussian, meaning that noise pulses are independent and they follow normal distribution. More general situation occurs when noise pulses follow α-stable law [17, 18]. The α-stable white noise is a generalization of the Gaussian white noise including the former as a special limiting case. α-stable noises are capable to describe out-of-equilibrium systems displaying heavy tailed fluctuations [17, 19–23]. Growing number of observations [24–30] demonstrates abundance of systems displaying more general fluctuations, *i.e.* the so-called Lévy flights. Consequently, noise-induced effects including stochastic resonance [31–34] and resonant activation [34–43] have been also explored in systems perturbed by Lévy noises.

Up to now, examination of the stochastic resonance focused on 1D systems mainly including Markovian and non-Markovian regimes [44] and their entropic extensions [45, 46]. Here, we make a next step, *i.e.* we extend the system spatial dimension to two. Consequently, after exploration of 2D problems: resonant activation [47], stationary states [48] and escape kinetics from bounded domains [49, 50], we explore properties of the stochastic resonance in a 2D system. The studied model not only advances examination of the stochastic resonance but also extends our understanding of stochastic dynamics of multidimensional systems. The studied setup, required theory and main results are presented in Model and results (Sec. 2). The paper is closed with Summary and discussion (Sec. 3).

2. Model and results

Let us consider a 2D motion of a particle subjected to the bi-variate α-stable Lévy-type noise

$$\frac{\mathrm{d}\boldsymbol{x}}{\mathrm{d}t} = -\nabla V(\boldsymbol{x}) + A_0 \sin(\Omega t)\hat{\boldsymbol{x}} + \sigma\boldsymbol{\zeta}_\alpha(t)\,. \tag{1}$$

Equation (1) can be rewritten as

$$\mathrm{d}\boldsymbol{x} = -\nabla V(\boldsymbol{x})\mathrm{d}t + A_0 \sin(\Omega t)\mathrm{d}t\hat{\boldsymbol{x}} + \sigma\mathrm{d}\boldsymbol{L}_\alpha(t)\,, \tag{2}$$

where $V(\boldsymbol{x})$ is a static, 2D double-well potential

$$V(x,y) = \frac{b}{4}x^4 - \frac{a}{2}x^2 + \frac{b}{4}y^4\,. \tag{3}$$

In Eq. (2), $\mathrm{d}\boldsymbol{L}_\alpha(t)$ represents stochastic integration with respect to the α-stable motion $\boldsymbol{L}_\alpha(t)$ [17] and $\hat{\boldsymbol{x}}$ is a unit vector along x-axis. In order

to maintain double-well type of the potential (3) parameters a and b need to be positive. Within the simulation, they have been set to $a = 128$, $b = 512$ and $A_0 = 8$. As in 1D, the bi-variate α-stable noise $\boldsymbol{\zeta}_\alpha(t)$ is a formal time derivative of the bi-variate α-stable motion $\boldsymbol{L}_\alpha(t)$. Therefore, increments $\Delta\boldsymbol{L}_\alpha(t) = \boldsymbol{L}_\alpha(t+\Delta t) - \boldsymbol{L}_\alpha(t)$ of the α-stable motion $\boldsymbol{L}_\alpha(t)$ are independent and distributed according to the bi-variate α-stable density, which has the characteristic function

$$\phi(\boldsymbol{k}) = \begin{cases} \exp\left\{-\int\limits_{S_d} |\langle \boldsymbol{k}, \boldsymbol{s}\rangle|^\alpha \left[1 - i\,\mathrm{sign}(\langle \boldsymbol{k}, \boldsymbol{s}\rangle) \tan\frac{\pi\alpha}{2}\right] \Lambda(\mathrm{d}\boldsymbol{s}) + i\left\langle \boldsymbol{k}, \boldsymbol{\mu}^0\right\rangle\right\} \\ \text{for } \alpha \neq 1\,, \\ \exp\left\{-\int\limits_{S_d} |\langle \boldsymbol{k}, \boldsymbol{s}\rangle| \left[1 + i\frac{2}{\pi}\mathrm{sign}(\langle \boldsymbol{k}, \boldsymbol{s}\rangle) \ln(\langle \boldsymbol{k}, \boldsymbol{s}\rangle)\right] \Lambda(\mathrm{d}\boldsymbol{s}) + i\left\langle \boldsymbol{k}, \boldsymbol{\mu}^0\right\rangle\right\} \\ \text{for } \alpha = 1\,, \end{cases} \tag{4}$$

where $\langle \boldsymbol{k}, \boldsymbol{s}\rangle$ represents the scalar product, $\Lambda(\cdot)$ stands for the spectral measure on the unit circle S_2 of $\mathbb{R}^2$ and $\boldsymbol{\mu}^0$ is a vector in $\mathbb{R}^2$, see [17]. The spectral measure $\Lambda(\cdot)$ replaces skewness and scale parameters which characterize 1D α-stable densities [17, 18]. Bi-variate α-stable density is said to be symmetric if the spectral measure is symmetric, see [17, 51, 52]. The bi-variate α-stable motion $\boldsymbol{L}_\alpha(t)$ can be generated by general methods described in [17, 53, 54].

The noise-driven dynamics of 2D systems perturbed by bi-variate α-stable noises is determined by the spectral measure $\Lambda(\cdot)$. Various choices of spectral measures result in different bi-variate α-stable noises and, consequently, in different (fractional) diffusion equations. Here, we use the uniform continuous spectral measure only. The uniform continuous spectral measure $\Lambda(\cdot)$ corresponds to the situation when α-stable densities are spherically symmetric, *i.e.* they depend on $|\boldsymbol{x}|$ only. In such a case, the Langevin equation (1) is associated with the following fractional diffusion equation [55–57]

$$\frac{\partial p(\boldsymbol{x}, t|\boldsymbol{x}_0, t)}{\partial t} = \nabla \cdot [\nabla V(\boldsymbol{x}, t) p(\boldsymbol{x}, t|\boldsymbol{x}_0, t))] - \sigma^\alpha (-\Delta)^{\alpha/2} p(\boldsymbol{x}, t|\boldsymbol{x}_0, t)\,, \tag{5}$$

where $-(-\Delta)^{\alpha/2}$ is the fractional Riesz–Weil derivative (Laplacian) defined via its Fourier transform [57]

$$\mathcal{F}[-(-\Delta)^{\alpha/2} p(\boldsymbol{x}, t|\boldsymbol{x}_0, t)] = -|\boldsymbol{k}|^\alpha \mathcal{F}[p(\boldsymbol{x}, t|\boldsymbol{x}_0, t)]$$

and $V(\boldsymbol{x}, t)$ is a time-dependent potential $V(x, y, t) = \frac{b}{4}x^4 - \frac{a}{2}x^2 + \frac{b}{4}y^4 - A_0 x \sin(\Omega t)\hat{\boldsymbol{x}}$. Consequently, the studied system is determined by a 2D potential and 2D noise with not independent components.

In order to measure the strength of stochastic resonance, one needs to rely on various measures. Most common are quantifiers based on power-spectra: signal-to-noise ratio or spectral power amplification [2]. Nevertheless, there are other measures which can be calculated without using Fourier methods, *e.g.* periodic response [2], area under the "first peak" of the residence time distribution [58] and probability of given number of transitions per period of the external modulation [59, 60]. Here, we verify applicability of these methods to systems perturbed by bi-variate α-stable noises. All mentioned measures are defined for 1D systems. Consequently, in order to use them, a bi-variate trajectory $\boldsymbol{x}(t)$ needs to be transformed into 1D signal. For example, instead of a full trajectory $\boldsymbol{x}(t) = (x(t), y(t)))$, one can use $x(t)$ only, *i.e.* the component of the full 2D trajectory which is parallel to the direction of the external periodic perturbation $A_0 \sin(\omega t)$.

The stochastic resonance is studied numerically by means of Monte Carlo methods. Main simulations were performed with the integration time step $\Delta t = 10^{-3}$ and averaged over $N = 10^4$ repetitions. Initially, a random walker was located in the $\boldsymbol{x}(0) = (-\sqrt{b/a}, 0)$ with $a = 128$ and $b = 512$, *i.e.* in the left potential well. The period, T_Ω, of the external modulation is $T_\Omega = 1$, *i.e.* $\Omega = 2\pi$ and its amplitude $A_0 = 8$.

Figures 1 and 2 present sample trajectories of the process $\boldsymbol{x}$ along with respective x-components, *i.e.* $x(t)$. With increasing value of the stability index α, long jumps become less probable and trajectories are more localized in the vicinity of minima of the 2D potential.

In the long time limit, the process $\boldsymbol{x}(t)$ looses the memory about its initial condition and $\langle x(t) \rangle$ becomes a periodic function of time

$$\langle x(t) \rangle = A_{\max} \sin(\Omega t + \phi)\,. \tag{6}$$

Therefore, the average position $\langle x(t) \rangle$ follows the periodicity T_Ω of the external periodic modulation $A_0 \sin(\Omega t)$. Figure 3 presents sample average position $\langle x(t) \rangle$ for various values of the stability index α (various panels) and different values of the scale parameter σ (various curves). For low values of the stability index α, larger fluctuations of average position are visible. Figure 3 demonstrates that, like in the classical stochastic resonance, changes in the scale parameter modify strength of the periodic response. This fact is further confirmed in Fig. 4 which presents amplitude of the periodic response $A_{\max}$, see Eq. (6), as a function of the scale parameter σ. The amplitude $A_{\max}$ depends in the non-monotonous way on the scale parameter, *i.e.* there exists an optimal value of the scale parameter σ for which the periodic response is the strongest. For low values of the stability index α, the optimal scale parameter can be very large. The location of the maximum of the periodic response $A_{\max}$ does not need to coincide with the point for which $\langle \tau \rangle = T_\Omega/2$, compare Figs. 4 and 5.

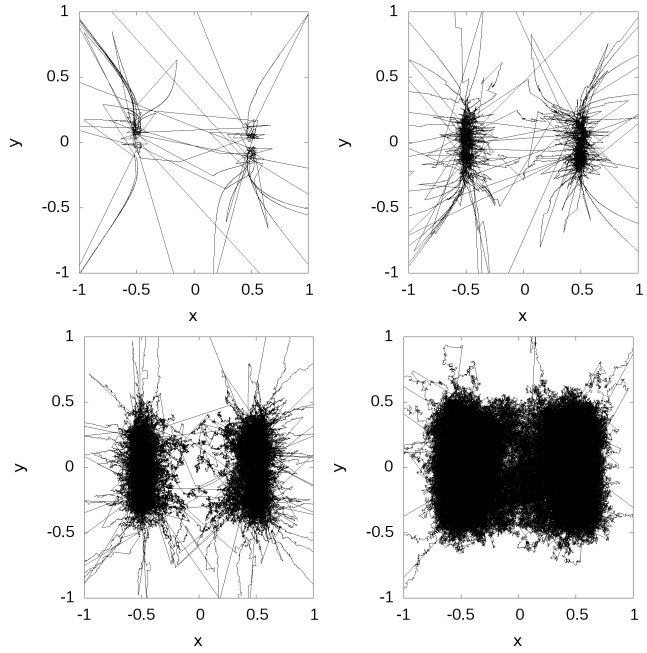

Fig. 1. Sample 2D trajectories for various values of the stability index α: $\alpha = 0.5$ (left top), $\alpha = 1.0$ (right top), $\alpha = 1.5$ (left bottom) and $\alpha = 1.9$ (right bottom). The scale parameter $\sigma = 3$.

The domain of motion and probability of visiting points in space are determined by the combined action of the deterministic force (potential) and random force (noise), see Fig. 1. The deterministic double-well bi-variate potential has two minima which define two states of the processes $\boldsymbol{x}(t)$. It can be assumed that the border between states is defined by the $x = 0$ line, *i.e.* when $x > 0$, the process is in the "right" state, while for $x < 0$, it is in the "left" state. Such definition introduces possibility of multiple recrossing events when $x \approx 0$. Therefore, in order to discriminate states in a robust way, it is necessary to introduce additional constraints. For example, it is possible to assume that a couple, let say two or four, consecutive values of $x(t)$ are at the same side of $x = 0$ line in order to assure transition between states. Here, we have used alternative approach. A transition between states takes place when a particle crosses $x = 0$ and reaches the vicinity of the another potential minimum. Such an approach produces results which are coherent with the former approach, see [35], due to the fact that motion to a minimum of the potential is significantly faster than surmounting the potential barrier.

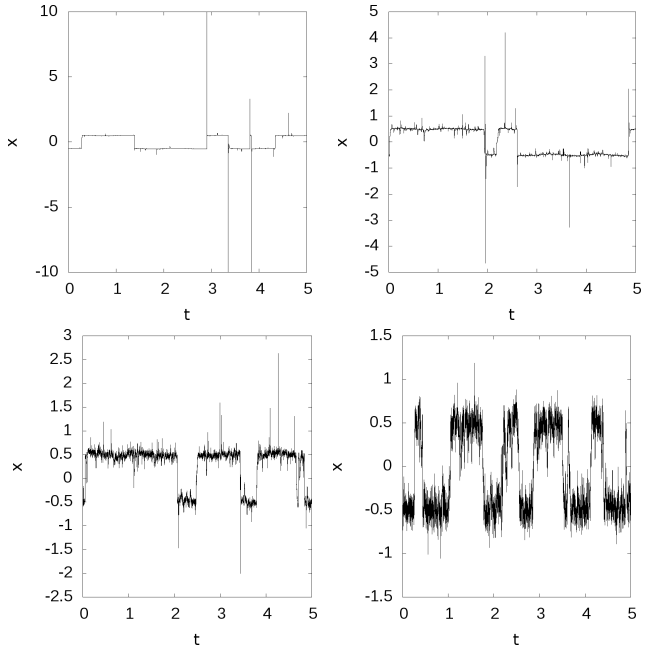

Fig. 2. x-components of sample 2D trajectories for various values of the stability index α: $\alpha = 0.5$ (left top), $\alpha = 1.0$ (right top), $\alpha = 1.5$ (left bottom) and $\alpha = 1.9$ (right bottom) corresponding to 2D trajectories from Fig. 1.

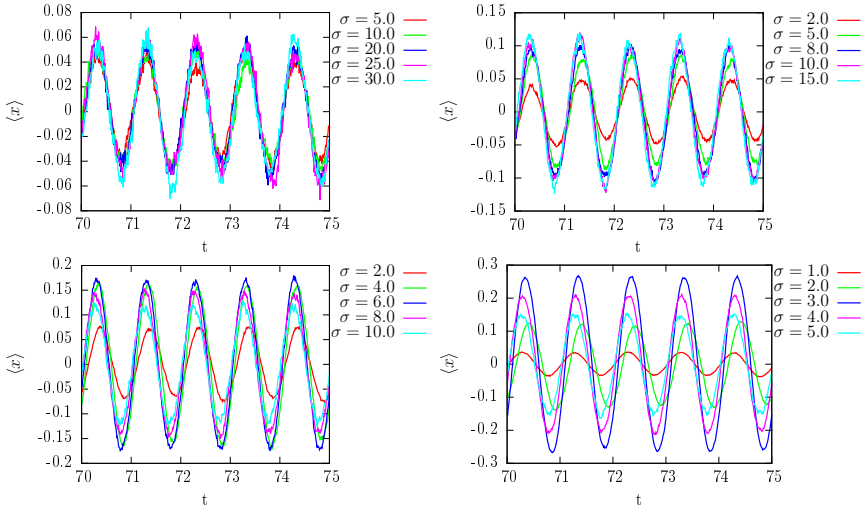

Fig. 3. Average position $\langle x \rangle$ for various values of the stability index α: $\alpha = 0.5$ (left top), $\alpha = 1.0$ (right top), $\alpha = 1.5$ (left bottom) and $\alpha = 1.9$ (right bottom). Various curves correspond to various values of the scale parameter σ.

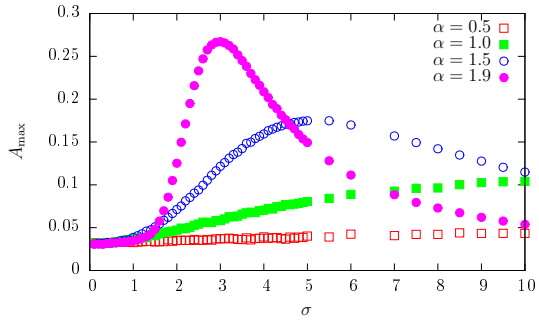

Fig. 4. Amplitude of the periodic response $A_{\max}$ as a function of the scale parameter σ. Various curves correspond to various values of the stability index α: 0.5, 1.0, 1.5 and 1.9.

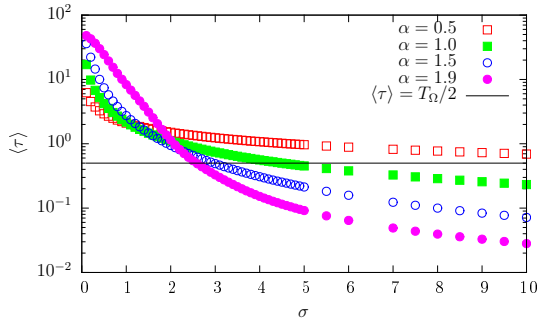

Fig. 5. The mean residence time in any of states for the escape from the periodically modulated potential (3), *i.e.* $V(\boldsymbol{x}) - A_0 x \sin(\Omega t)\hat{\boldsymbol{x}}$. Various curves correspond to various values of the stability index α.

Figure 5 presents the average residence time for both (left and right) states, *i.e.* it is the average of time intervals τ between transitions from a state to the other state. The mean residence time is a decreasing function of the scale parameter σ. This is the direct consequence of the fact that if the noise pulses are distributed according to a distribution with larger scale parameter σ, transitions between states occur more often. More intriguing is the role of the stability index α. For low values of the scale, parameter σ decrease of the stability index α accelerates escape kinetics (lowers the mean residence time). In the opposite limit of large values of the scale parameter, the mean residence time is an decreasing function of the stability index α. This indicates non-trivial interplay between the scale parameter (width of the distribution) and the stability index (tails of the distribution). The solid line in Fig. 5 shows $\langle\tau\rangle = T_\Omega/2 = 1/2$ condition. This line demonstrates where a simple condition of the stochastic resonance $\langle\tau\rangle = T_\Omega/2$ is fulfilled,

i.e. when, on average, a particle can switch between states during a half of the modulation period [2]. Putting it differently, it shows when there is the best synchronization between the external driving and the particle position $x(t)$.

Next possibility to quantify the stochastic resonance is to use the residence time distributions [2, 58]. Residence time distribution is sensitive to the barrier modulation process because escape events are most likely to take place when the relative height of the barrier separating minima is the lowest. Therefore, one can expect that the particle jumps from the left to the right state when the relative barrier height is minimal. Then, it waits half a driving period in the right state for the optimal returning possibility. Consequently, after a whole driving period, the well-synchronized particle returns to the initial potential well, while jumps are performed over the lowest possible relative barrier heights. In cases of worse synchronizations, particle waits for optimal opportunities which occur every period of the driving force. Therefore, in the Gaussian stochastic resonance, residence time distributions show clear peaks at $(n+1/2)T_\Omega$, where $n = 0, 1, 2, \ldots$ The $n = 0$ peak is the one fulfilling the condition $\langle\tau\rangle = T_\Omega/2$. Sample residence time distributions are plotted in Fig. 6. The multi-modality of the residence time distribution disappears with decrease of the stability index α. The reminiscence of this tendency is visible for $\alpha = 1.9$. For smaller values of the stability index α,

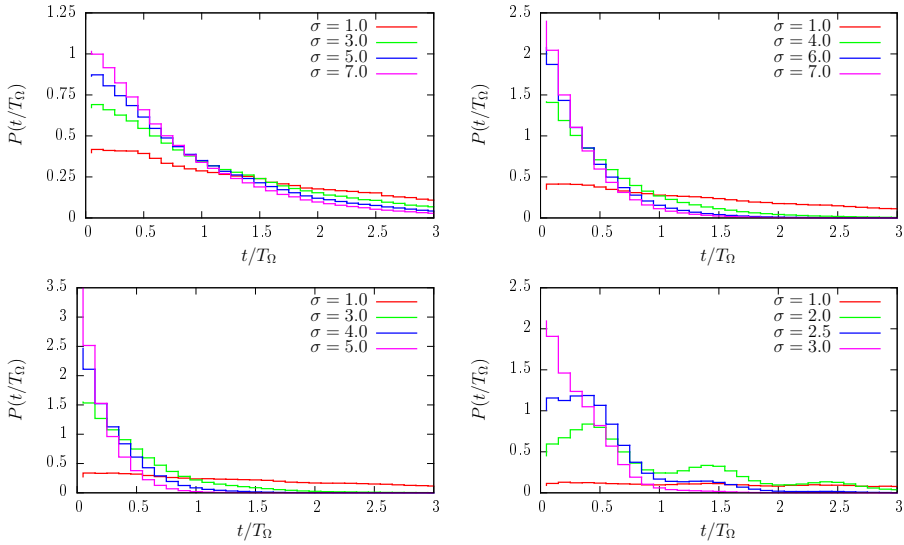

Fig. 6. Residence time distributions, *i.e.* $P(t/T_\Omega)$ for various values of the stability index α: $\alpha = 0.5$ (left top), $\alpha = 1.0$ (right top), $\alpha = 1.5$ (left bottom) and $\alpha = 1.9$ (right bottom). Various curves correspond to various values of the scale parameter σ.

noise induced fluctuations of $x(t)$ are large enough to destroy multi-peaked dependence of the residence time distribution. Nevertheless, the area S_1 under the "first peak"

$$S_1 = \int_{0.25}^{0.75} P(t/T_\Omega)\mathrm{d}t \tag{7}$$

displays typical, non-monotonous dependence on the scale parameter σ. Figure 7 presents the area S_1 calculated according to Eq. (7). Integration limits in Eq. (7) are shifted in comparison to $[0, T_\Omega/2]$ in order to remove the bias introduced by the exponential background of the residence time distribution. Optimal values of the scale parameter σ are coherent with results presented in Fig. 5 because the mean residence time $\langle\tau\rangle$ is related to the residence time distribution.

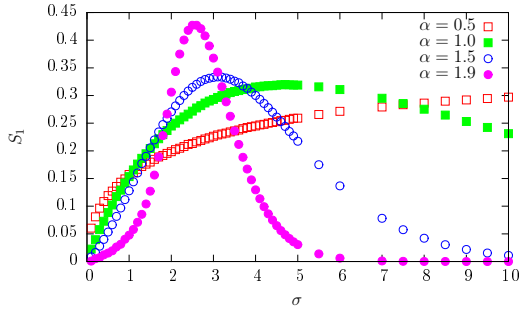

Fig. 7. Area under the "first peak" of the residence time distribution, *i.e.* $\int_{0.25}^{0.75} P(t/T_\Omega)\mathrm{d}t$, as a function of the scale parameter σ. Various curves correspond to various values of the stability index α: 0.5, 1.0, 1.5 and 1.9.

Finally, Fig. 8 presents a probability of given number of transitions per period of the external modulation which can be also used to detect the stochastic resonance. According to this measure, the stochastic resonance is observed when a probability of two transitions, $P(2)$, per period of the external driving is maximal. Such a definition is coherent with the intuitive criterion of the stochastic resonance, *i.e.* $\langle\tau\rangle = T_\Omega/2$ because two transitions means that average residence time in any of potential wells is $T_\Omega/2$, compare top panel of Fig. 8 with Figs. 5 and 7. Subsequent (middle and bottom) panels of Fig. 8 present probability of three ($P(3)$) and four ($P(4)$) transitions per period of the external modulation. Maxima of $P(3)$ and $P(4)$ are observed for larger values of the scale parameter σ than the maximum of $P(2)$ due to the fact that larger scale parameter facilitates escape kinetics. This is further manifested by the decay of the mean residence time with the increase of σ, see Fig. 5.

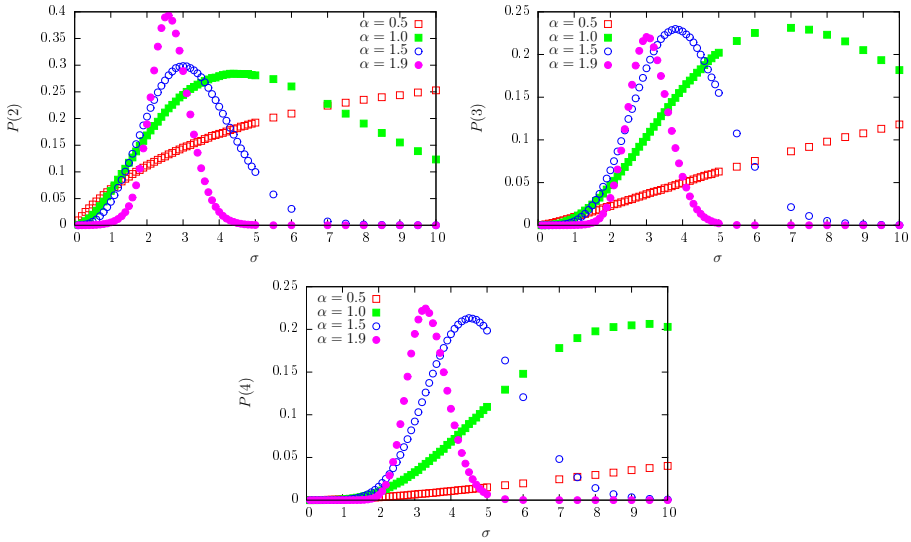

Fig. 8. Probability of given number of transitions per period $T_\Omega = 2\pi/\Omega$ of the external driving force as a function of the scale parameter σ. Various panels correspond to different number of transitions from 2 to 4 (from top left to bottom). Various curves correspond to various values of the stability index α: 0.5, 1.0, 1.5 and 1.9.

Table I summarizes main information about quantifiers of the stochastic resonance. In particular, it shows values of the scale parameter σ for which the condition $\langle\tau\rangle = T_\Omega/2$ is fulfilled. Moreover, it presents optimal values of the scale parameter resulting in maximal values of the periodic response ($A_{\max}$), area under the "first peak" of the residence time distribution (S_1) and probability of given number of transitions per period of the external driving

TABLE I

Values of the scale parameters optimizing (maximizing) various criteria of the stochastic resonance: periodic response ($A_{\max}$), area under the "first peak" of the residence time distribution (S_1) and probability of a given number of transitions ($P(2), P(3), P(4)$).

α	$\langle\tau\rangle = T_\Omega/2$	$A_{\max}$	S_1	$P(2)$	$P(3)$	$P(4)$
1.9	2.6	3.0	2.6	2.6	3	3.3
1.5	3	5.0	3.1	3	4.1	4.5
1.0	4.5	10.0	4.7	4.4	7	9.5
0.5	20	8.5	20	20	30	30

T_Ω ($P(2), P(3)$ and $P(4)$). Among applied stochastic resonance quantifiers, only the periodic response does not use the information about the state of the processes. Remaining measures (including $\langle\tau\rangle = T_\Omega/2$ condition) rely on the discrimination between states. As it can be deducted from Table I, the condition $\langle\tau\rangle = T_\Omega/2$ and quantifiers S_1 and $P(2)$ give quantitatively similar values of the optimal scale parameter. The periodic response $A_{\max}$ gives significantly different results than other measures used.

3. Summary and conclusions

Using extensive computer simulations, it has been shown that in a two-dimensional system driven by bi-variate α-stable noise stochastic resonance can be successfully detected. As a model, we have used the 2D analog of 1D double-well potential, $V(x,y) = \frac{b}{4}x^4 - \frac{a}{2}x^2 + \frac{b}{4}y^4$ which is subjected to the additional external periodic modulation $A_0 x \sin(\Omega t)\hat{\boldsymbol{x}}$. Due to the form of the potential, the deterministic force acting on a particle separates into independent parts acting along both axes. This, however, does not reduce the problem to a one-dimensional one for the x-direction, since the projections of bi-variate isotropic α-stable noises on the axes result in one-dimensional α-stable noises, which are not independent. Consequently, the dimensionality of the system cannot be reduced, although the dependence between the components of particle position $x(t)$ and $y(t)$ is introduced by a bi-variate α-stable noise only. For this system, we demonstrated that periodic response, area under the "first peak" of the residence time distribution and probability of given number of transitions per period of the external driving are perfectly applicable for detection of the stochastic resonance driven by α-stable noises. These quantifiers provide robust measures of the stochastic resonance which can be used in systems displaying heavy-tailed fluctuations.

This project was supported in part by the grant from the Polish National Science Center (2014/13/B/ST2/02014) and by the DFG grant SO 307/4-1. Computer simulations have been performed at the Academic Computer Center Cyfronet, Akademia Górniczo-Hutnicza (Kraków, Poland) under CPU grant MNiSW/Zeus_lokalnie/UJ/052/2012.

REFERENCES

[1] B. McNamara, K. Wiesenfeld, *Phys. Rev. A* **39**, 4854 (1989).

[2] L. Gammaitoni, P. Hänggi, P. Jung, F. Marchesoni, *Rev. Mod. Phys.* **70**, 223 (1998).

[3] V.S. Anishchenko, A.B. Neiman, F. Moss, L. Schimansky-Geier, *Sov. Phys. Usp.* **42**, 7 (1999).

[4] L. Gammaitoni, P. Hänggi, P. Jung, F. Marchesoni, *Eur. Phys. J. B* **69**, 1 (2009).

[5] C.R. Doering, J.C. Gadoua, *Phys. Rev. Lett.* **69**, 2318 (1992).

[6] A.A. Dubkov, N.V. Agudov, B. Spagnolo, *Phys. Rev. E* **69**, 061103 (2004).

[7] V.S. Anishchenko, A.B. Neiman, in: *Stochastic Dynamics*, edited by L. Schimansky-Geier, T. Pöshel, Springer Verlag, Berlin 1997, p. 155.

[8] R. Benzi, G. Parisi, A. Sutera, A. Vulpiani, *Tellus* **34**, 10 (1982).

[9] K. Wiesenfeld, F. Moss, *Nature (London)* **373**, 33 (1995).

[10] A. Fuliński, *Chaos* **8**, 549 (1998).

[11] D.F. Russell, L.A. Wilkens, F. Moss, *Nature* **402**, 291 (1999).

[12] P. Hänggi, *ChemPhysChem* **3**, 285 (2002).

[13] A.A. Priplata *et al.*, *Phys. Rev. Lett.* **89**, 238101 (2002).

[14] A.A. Priplata *et al.*, *Lancet* **362**, 1123 (2003).

[15] M. Costa *et al.*, *Europhys. Lett.* **77**, 68008 (2007).

[16] O. Kaut *et al.*, *Neurorehabilitation* **28**, 353 (2011).

[17] G. Samorodnitsky, M.S. Taqqu, *Stable Non-Gaussian Random Processes: Stochastic Models with Infinite Variance*, Chapman and Hall, New York 1994.

[18] A. Janicki, A. Weron, *Simulation and Chaotic Behavior of α-stable Stochastic Processes*, Marcel Dekker, New York 1994.

[19] R. Metzler, J. Klafter, *Phys. Rep.* **339**, 1 (2000).

[20] A.V. Chechkin, V.Y. Gonchar, J. Klafter, R. Metzler, *Adv. Chem. Phys.* **133**, 439 (2006).

[21] R. Klages, G. Radons, I.M. Sokolov, *Anomalous Transport: Foundations and Applications*, Wiley-VCH, Weinheim 2008.

[22] A.A. Dubkov, B. Spagnolo, V.V. Uchaikin, *Int. J. Bifur. Chaos. Appl. Sci. Eng.* **18**, 2649 (2008).

[23] R. Metzler, A.V. Chechkin, V.Y. Gonchar, J. Klafter, *Chaos Solitons Fractals* **34**, 129 (2007).

[24] *Lévy Flights and Related Topics in Physics*, edited by M.F. Shlesinger, G.M. Zaslavsky, J. Frisch, Springer Verlag, Berlin 1995.

[25] *Lévy Processes: Theory and Applications*, edited by O.E. Barndorff-Nielsen, T. Mikosch, S.I. Resnick, Birkhäuser, Boston 2001.

[26] P.D. Ditlevsen, *Geophys. Res. Lett.* **26**, 1441 (1999).

[27] R.N. Mantegna, H.E. Stanley, *An Introduction to Econophysics. Correlations and Complexity in Finance*, Cambridge University Press, Cambridge 2000.

[28] T.H. Solomon, E.R. Weeks, H.L. Swinney, *Phys. Rev. Lett.* **71**, 3975 (1993).

[29] A.V. Chechkin, V.Y. Gonchar, M. Szydłowski, *Phys. Plasmas* **9**, 78 (2002).

[30] S. Boldyrev, C.R. Gwinn, *Phys. Rev. Lett.* **91**, 131101 (2003).

[31] B. Kosko, S. Mitaim, *Phys. Rev. E* **64**, 051110 (2001).
[32] D. Applebaum, *IEEE Trans. Neural Networks* **20**, 1993 (2009).
[33] B. Dybiec, *Phys. Rev. E* **80**, 041111 (2009).
[34] B. Dybiec, E. Gudowska-Nowak, *J. Stat. Mech.* **2009**, P05004 (2009).
[35] B. Dybiec, E. Gudowska-Nowak, *Acta Phys. Pol. B* **38**, 1759 (2007).
[36] B. Dybiec, E. Gudowska-Nowak, *Phys. Rev. E* **69**, 016105 (2004).
[37] B. Dybiec, E. Gudowska-Nowak, P. Hänggi, *Phys. Rev. E* **75**, 021109 (2007).
[38] T. Munakata, T. Kawakatsu, *Progr. Theor. Phys.* **74**, 262 (1985).
[39] B.C. Bag, *Eur. Phys. J. B* **34**, 115 (2003).
[40] P. Hänggi, *Chem. Phys.* **180**, 157 (1994).
[41] J. Iwaniszewski, *Phys. Rev. E* **68**, 027105 (2003).
[42] T. Novotný, P. Chvosta, *Phys. Rev. E* **63**, 012102 (2000).
[43] P. Majee, G. Goswami, B.C. Bag, *Chem. Phys. Lett.* **416**, 256 (2005).
[44] I. Goychuk, P. Hänggi, *Phys. Rev. Lett.* **91**, 070601 (2003).
[45] P.S. Burada *et al.*, *Phys. Rev. Lett.* **101**, 130602 (2008).
[46] P.S. Burada *et al.*, *Europhys. Lett.* **87**, 50003 (2009).
[47] K. Szczepaniec, B. Dybiec, *J. Stat. Mech.* **2014**, P09022 (2014).
[48] K. Szczepaniec, B. Dybiec, *Phys. Rev. E* **90**, 032128 (2014).
[49] K. Szczepaniec, B. Dybiec, *J. Stat. Mech.* **2015**, P06031 (2015).
[50] B. Dybiec, K. Szczepaniec, *Eur. Phys. J. B* **88**, 1 (2015).
[51] M. Teuerle, A. Jurlewicz, *Acta Phys. Pol. B* **40**, 1333 (2009).
[52] M. Teuerle, P. Żebrowski, M. Magdziarz, *J. Phys. A: Math. Gen.* **45**, 385002 (2012).
[53] R. Modarres, J.P. Nolan, *Comput. Stat.* **9**, 11 (1994).
[54] J.P. Nolan, in: *A Practical Guide to Heavy Tails: Statistical Techniques and Applications*, edited by R.J. Feldman, M.S. Taqqu, Birkhäuser, Boston 1998, pp. 509–525.
[55] V.V. Yanovsky, A.V. Chechkin, D. Schertzer, A.V. Tur, *Physica A* **282**, 13 (2000).
[56] D. Schertzer *et al.*, *J. Math. Phys.* **42**, 200 (2001).
[57] S.G. Samko, A.A. Kilbas, O.I. Marichev, *Fractional Integrals and Derivatives. Theory and Applications*, Gordon and Breach Science Publishers, Yverdon 1993.
[58] L. Gammaitoni, F. Marchesoni, S. Santucci, *Phys. Rev. Lett.* **74**, 1052 (1995).
[59] P. Talkner *et al.*, *New J. Phys.* **7**, 14 (2005).
[60] C. Schmitt, B. Dybiec, P. Hänggi, C. Bechinger, *Europhys. Lett.* **74**, 937 (2006).